Journal of Applied Physics

Vibrational detection of delamination in composites using a combined finite element analysis and machine learning approach

Cite as: J. Appl. Phys. **128**, 125104 (2020); https://doi.org/10.1063/5.0015648
Submitted: 29 May 2020 . Accepted: 07 September 2020 . Published Online: 22 September 2020

Eric W. Jacobs, Charles Yang, Kahraman G. Demir, and Grace X. Gu

Journal of Applied Physics ARTICLE scitation.org/journal/jap

Vibrational detection of delamination in composites using a combined finite element analysis and machine learning approach

Cite as: J. Appl. Phys. 128, 125104 (2020); doi: 10.1063/5.0015648
Submitted: 29 May 2020 · Accepted: 7 September 2020 ·
Published Online: 22 September 2020

View Online Export Citation CrossMark

Eric W. Jacobs,[1] Charles Yang,[1,2] Kahraman G. Demir,[1] and Grace X. Gu[1,a)]

AFFILIATIONS

[1]Department of Mechanical Engineering, University of California, Berkeley, California 94720, USA
[2]Department of Electrical Engineering and Computer Science, University of California, Berkeley, California 94720, USA

Note: This paper is part of the special collection on Machine Learning for Materials Design and Discovery
[a)]**Author to whom correspondence should be addressed:** ggu@berkeley.edu

ABSTRACT

One common challenge of using composite materials is detecting delamination failure in a non-destructive and cost-effective way. Past studies have proven the feasibility of using vibrational measurements to detect damage but have not explored the full capabilities and limitations of vibrational testing. Here, we use a finite element model of a composite plate to characterize the natural frequency, mode shape, and mode curvature tests for a variety of delamination scenarios. We find that the mode curvature test is resource-intensive to conduct but provides the best resolution in both identifying and localizing delamination. On the other hand, the natural frequency test is simple and inexpensive to conduct but can only reliably identify the presence of delamination. Additionally, a machine learning model is implemented to augment the natural frequency test, allowing both localization of damage and quantification of its severity with only the natural frequencies of modes 1–6. We are able to interpret our model and discover a phase transition for natural frequencies with different sized delaminations. This testing framework allows rapid non-destructive analysis for the iterative design of composites, accelerating the development of novel delamination-resistant materials.

I. INTRODUCTION

Fiber-reinforced composites are commonly used in a variety of applications requiring high specific strength and stiffness, long fatigue life, and corrosion resistance. Although composite materials offer many advantages over traditional engineering materials,[1–5] their complex structure introduces numerous potential failure modes such as delamination, which occurs when individual plies of a laminate separate.[6] This type of damage can be difficult to detect because it is often invisible from the exterior of the structure. Yet, delamination can have detrimental effects on the mechanical properties of the material, potentially leading to catastrophic failure.[6–8]

Significant work has gone into developing noninvasive tools to detect delamination, including tap testing, x-ray imaging, ultrasonic imaging, and flash thermography,[9] but all of these methods have drawbacks. Furthermore, these tests only measure a specific area at a time, so small delaminated regions can easily be missed on large structures.[9] In this work, we explore the capabilities of vibrational methods, a class of testing with many advantages over conventional delamination testing. Many types of vibrational tests exist but they all rely on the same basic principle. Delamination within a laminate causes a local reduction in stiffness, which in turn changes the natural frequencies and mode shapes of the material.[10] This type of testing is attractive because it can be conducted rapidly using common inexpensive sensors, such as accelerometers. Furthermore, vibration captures the global behavior of the material, so vibrational methods have the potential to analyze an entire structure at once, unlike conventional testing methods that only measure a local region.[6] For many high-performance applications, there is an increasing demand for tailored composite materials that are able to resist delamination under extreme conditions. The speed of vibrational testing allows the rapid evaluation of novel materials, accelerating the design process. As vibrational methods become more sophisticated and robust, they will likely continue to see increased usage in a variety of industries.

A guide for classifying damage identification systems, developed by Rytter,[11] divides test methods into four levels based on their ability to identify, localize, and quantify damage. The four levels are defined as follows: level (1) identify the presence of a delaminated region; level (2) identify the location of a delaminated region; level (3) identify the location and severity of a delaminated region; and level (4) predict the remaining life based on the severity of a delaminated region. Most vibrational tests fall into level 1 or level 2, however, advancements in more complex vibrational methods allow for level 3 damage detection. Here, we focus on three of the most common vibrational tests—natural frequency, mode shape, and mode curvature. All three of these tests are forms of modal analysis but vary by what type of data is collected and analyzed.

For the natural frequency test, a structure is excited to vibrate, and the natural frequencies are measured and compared to the natural frequencies of a corresponding undamaged structure. A decrease in natural frequency is indicative of a reduction in stiffness caused by internal damage.[9,12] The simplicity of this test typically limits it to level 1 identification. The mode shape test involves measuring the shape of the natural frequency vibrational modes and comparing them against the modes of an undamaged structure. Żak *et al.*[13] showed that higher frequency modes of delaminated structures can contain distinct local behavior at the damaged region, allowing level 2 identification. This phenomenon is called delamination breathing and occurs when vibration drives the delamination open and closed.[6] This work focuses only on qualitative mode comparison though many researchers[14–16] have devised quantitative methods for comparing mode shapes. Finally, the mode curvature test uses modal displacements to calculate the geometric curvature of the vibrating structure.[9] Pandey *et al.*[17] showed that changes to mode curvature are a strong indicator of delamination, allowing level 2 or 3 identification. Calculating curvature can be difficult, however, and the corresponding damage plots often have a large amount of noise, obscuring interpretation.[18]

Machine learning models have demonstrated the ability to extract insights from noisy, high-dimensional information.[19–23] For instance, machine learning models have been used for phase reconstruction,[24] accelerated prediction of mechanical properties for composite designs,[25–27] and characterization of elastoplastic mechanical properties of materials.[28] Various machine learning methods have also been utilized specifically for non-destructive material testing, including support vector machines[29] and artificial neural networks.[30,31] However, while such methods often perform well, they tend to lack the capability for human analysis, that is, for the engineer to learn alongside the model. In other applications, random forests (RFs)[32] have shown themselves to be particularly well suited to tabular data and are often relatively easy to interpret.[33] Model interpretability of a non-destructive testing algorithm would allow engineers to learn from the model and gain new insight into material characterization. Here, we use random forests to characterize delaminations in composites using only the natural frequencies of the structure. This enables us to use cheaper, non-destructive methods to characterize composite designs, allowing a faster experimental feedback loop for the iterative design of novel composites. In addition, we are able to interpret our random forest model and identify novel relationships between natural frequencies and mode shapes.

In this work, we characterize the three aforementioned vibrational tests—natural frequency, mode shape, and mode curvature—in greater depth, allowing for a better understanding of their capabilities and limitations. A finite element model of a composite plate is used to explore two key parameters: delamination size and delamination location. Finite element analysis is well suited for this type of study because it allows rapid evaluation of a wide range of parameter combinations, allowing each test to be evaluated on its ability to detect and localize damage. In addition to simulation data, the practical considerations of conducting each test are analyzed to provide recommendations on use cases for each type of vibrational test. Finally, we demonstrate that machine learning is able to extract information about the delamination from the simpler, cheaper, natural frequency test, elevating it from level 1 to level 3 detection. We also interpret what the model has learned and discover a new phase transition in natural frequencies, confirmed with computational experiments.

II. METHODS

A. Computational model

In order to characterize the performance of the three vibrational tests, finite element simulations are run on a composite plate model with delaminations of varying size and location. These simulations are conducted in ANSYS using the modal analysis module. The composite model is constructed by stacking a series of solid unidirectional-fiber plies with stacking sequence $[0/90]_{2s}$. The composite material used is T300/934 graphite/epoxy with density $\rho = 1480\,\mathrm{kg/m^3}$, Young's moduli $E_{11} = 134$ GPa and $E_{22} = 10.3$ GPa, shear modulus $G_{12} = 5.0$ GPa, and Poisson's ratio $\nu_{12} = 0.33$ from Ref. 6. Unidirectional properties are defined using an orthotropic material model with ten material constants. However, the plies are transversely orthotropic and, thus, three constants are eliminated. Although out-of-plane properties are unknown for T300/934, they have little effect in this simulation and, thus, are estimated to equal in-plane properties. Each ply is meshed with a single layer of $8 \times 8\,\mathrm{mm}^2$ hexahedral elements. Plies are bonded together using a "bonded" type contact with multi-point constraint (MPC) formulation. Delaminations are created by defining unbonded rectangular zones on the faces of two adjacent plies and are notated by their ply interface (e.g., 1–2).

B. Verification with experimental results

To ensure the validity of the finite element model, experimental results from Shen and Grady[34] are compared with corresponding simulations according to the specifications used in their study. Three cases are tested for a $127 \times 12.7 \times 1.27\,\mathrm{mm}^3$ composite beam. First, an undamaged beam is tested. Then, a beam with a 50.8 mm delamination is tested. Finally, a beam with a 101.6 mm delamination is tested. The delaminations are centered and extend through the full width of the beam. One side of the beam is defined as a fixed constraint, and modal analysis is conducted. For each simulation, the natural frequency of the first mode is extracted.

C. Parameter testing

In order to characterize the ability of vibrational tests to identify and localize delaminations, three parameters—delamination size, delamination ply interface, and delamination location in the x-axis—are tested on a $200 \times 200 \times 2\,\text{mm}^3$ composite plate. One end of the plate is defined as a fixed constraint and modal analysis is conducted. Figure 1 shows the laminate model setup with numbered plies. The first set of simulations are conducted to measure the effect of delamination size. Delaminations between ply 4 and ply 5 (4–5) centered at $x = 100$ mm are tested with lengths varying between 5 mm and 150 mm. The second round of simulations are conducted to measure the effect of ply interface. Delaminations between ply 1 and ply 2 (1–2) centered at $x = 100$ mm are tested with lengths also varying between 5 mm and 150 mm. The final set of simulations are conducted to measure the effect of the x-axis location. Delaminations (4–5) of varying sizes centered at $x = 50$, 100, and 150 mm are tested. All delamination parameter combinations for these tests are shown in Table I.

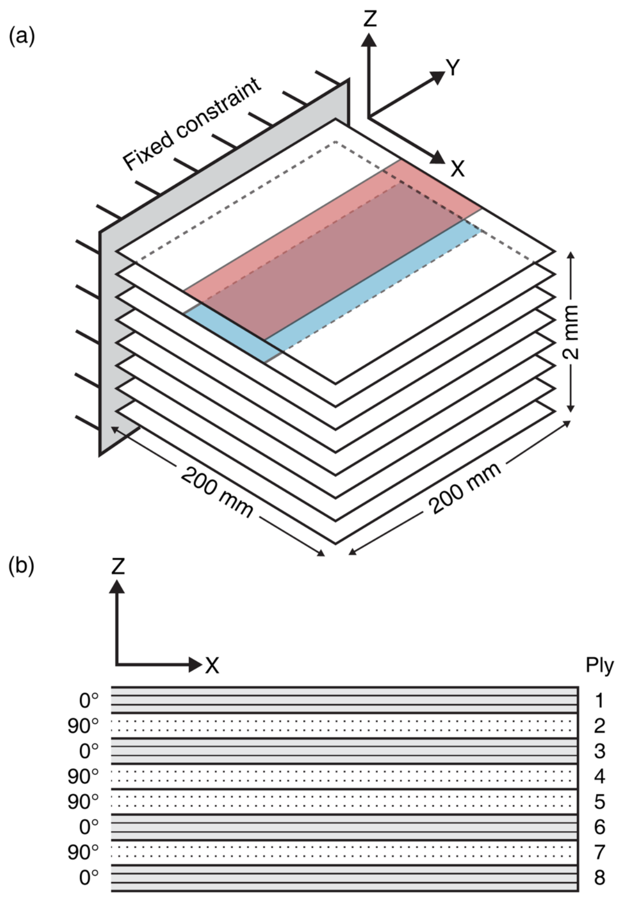

FIG. 1. (a) Exploded view of the model showing the coordinate system, fixed edge, and 1–2 delamination extending across the width of the plate. (b) Laminate stack showing ply numbering and fiber orientations.

TABLE I. Parameter combinations used for parameter testing simulations.

Ply interface	x-axis location (mm)	Delamination size (mm × mm)
4–5	100	5, 10, 20, 40, 60, 80, 100, 125, 150 × 200
1–2	100	5, 10, 20, 40, 60, 80, 100, 125, 150 × 200
4–5	50, 100, 150	10, 20, 40, 80 × 200

After each simulation is run, results are gathered for each test type. First, natural frequencies corresponding to modes 1–6 are extracted. Then, top-down views of modes 1–4 are captured. Finally, the displacements of mesh nodes on the top surface of the plate are extracted for mode 1. Curvature is calculated using Eq. (1), where κ is the curvature and v is the displacement in the z-axis.[35] Data are numerically differentiated using the Laplacian difference method,[36]

$$\kappa = \frac{\partial^2 v}{\partial x^2}. \tag{1}$$

D. Machine learning

To train the machine learning model, a data set is generated by running 6000 simulations with randomly generated rectangular delaminations. For each simulation, the side lengths of the delaminated region are each randomly generated from a uniform distribution between 2 mm and 196 mm. Then, the x and y coordinates of the center of the delamination are randomly generated, ensuring the edges of the delamination are at least 2 mm from the edges of the plate. Additionally, the simulations cover all four ply interfaces rather than just 1–2 and 4–5 with 1500 simulations run for each interface. We use a random forest (RF) model—due to its excellent performance on tabular data and good generalizability—to predict the area of the delamination and the distance from the boundary condition, given only the first six natural frequency modes.[32] In brief, random forests construct an ensemble of decision trees, where each decision tree only sees a bootstrap sample of the entire data set. This prevents any individual decision tree from overfitting, but by taking the average of the predictions of the decision trees in the forest, the random forest model makes accurate predictions in a manner analogous to "wisdom of the crowd." For our implementation, we use the model provided in scikit-learn with 20 decision trees in each random forest.[37] The model is fit on the data set of 6000 simulations and their corresponding natural frequencies from modes 1–6 with a train/test split of 80/20. The model training computation time is 6.8 s, and the total prediction computation time is 0.09 s run on an Intel i7-7500 U CPU with 1 core. In order to interpret the random forest, we use the tree-interpreter package, which converts a prediction by the random forest into a linear model. The linear weight for each feature is the change in average output value at the decision nodes associated with that feature along the decision path.[33]

TABLE II. Comparison of simulation and experimental (Ref. 34) results for mode 1 natural frequency.

Delamination	Simulation (Hz)	Experiment (Hz)	Error (%)
Undamaged	81.9	79.8	2.6
50.8 mm	76.3	75.4	1.2
101.6 mm	57.0	57.5	0.9

III. RESULTS

A. Verification with experimental results

To verify our simulations, we compare our simulation results with experimental results from Shen and Grady. The results of the experimental verification with Shen and Grady are shown in Table II. For each of the three cases tested, the natural frequency determined from modal simulation matches the experimentally measured natural frequency to within 3%. Accuracy further improves to within 1% for large delaminations. These results demonstrate the validity of the finite element model over a wide range of damage. Although the experimental tests only measure mode 1, a past study by Zhang *et al.*[10] demonstrated good experimental agreement up to mode 7 with a similar composite finite element model, boundary conditions, and laminate geometry. Therefore, it is believed that matching experimental results for mode 1 is sufficient to ensure the accuracy of the model.

B. Natural frequency

The first two sets of simulations are conducted to analyze the ability of the natural frequency test to detect delaminations of different sizes and ply interfaces. Figure 2(a) shows the normalized frequencies of modes 1–6 over a range of delamination sizes in the 4–5 and 1–2 interfaces. For both 4–5 and 1–2 delaminations, the natural frequencies of all modes decrease as delamination size increases, consistent with theoretical predictions. For 4–5 delaminations, the frequencies of all modes decrease at roughly the same rate, except for mode 6 which decreases slightly faster. However, for 1–2 delaminations, the frequencies of modes 3–6 decrease significantly faster than the lower modes, particularly at large delamination sizes. As noted by Salawu,[14] a frequency change of about 5% is required to reliably detect damage. Therefore, the natural frequency test can detect delaminations of a normalized length of roughly 0.3 using modes 1–6.

The third set of simulations is conducted to analyze the ability of the natural frequency test to localize damage in the x-axis. Figure 2(b) shows the normalized frequency of mode 1 over a range of delamination sizes centered at $x = 0.25$, 0.50, and 0.75. Following the previous trend, the natural frequency decreases as the delamination size increases. However, for delaminations of comparable size, there is a difference in natural frequency based on the location in the x-axis. The frequency drop occurs more rapidly in delaminations closer to the fixed edge and less rapidly in delaminations closer to the free edge. This implies the possibility of localizing damage with natural frequencies. However, using a single mode creates ambiguity: a small delamination close to the fixed edge and a large delamination close to the free edge may have the same natural frequency.

C. Mode shape

For each simulation, top-down views of modes 1–4 are captured for qualitative comparison. The plots are colored with a blue–red scale, with blue corresponding to low displacement and red corresponding to high displacement. The exact numeric value of these displacements is not important for qualitative comparison

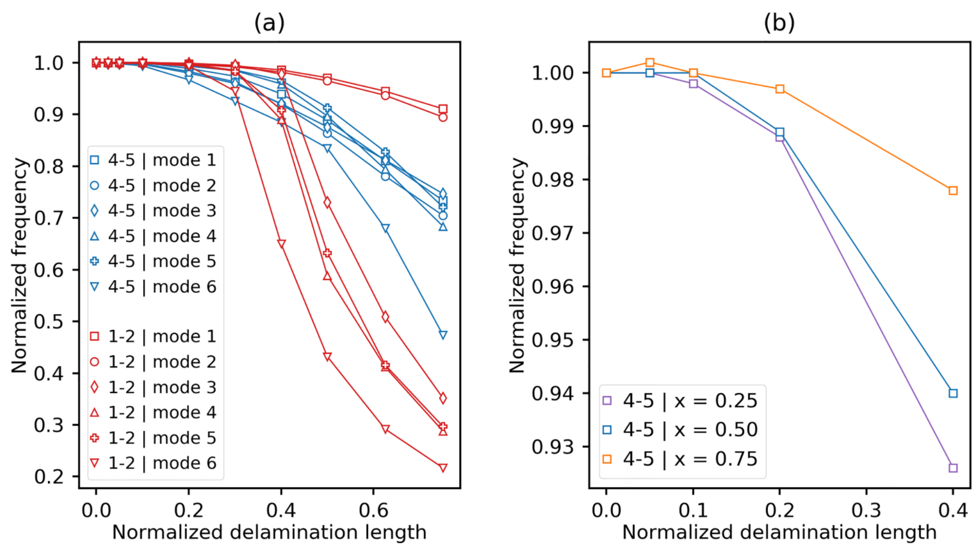

FIG. 2. (a) Mode 1–6 natural frequencies of 4–5 and 1–2 delaminations at $x = 0.50$. (b) Mode 1 natural frequencies of 4–5 delaminations at $x = 0.25$, 0.50, and 0.75.

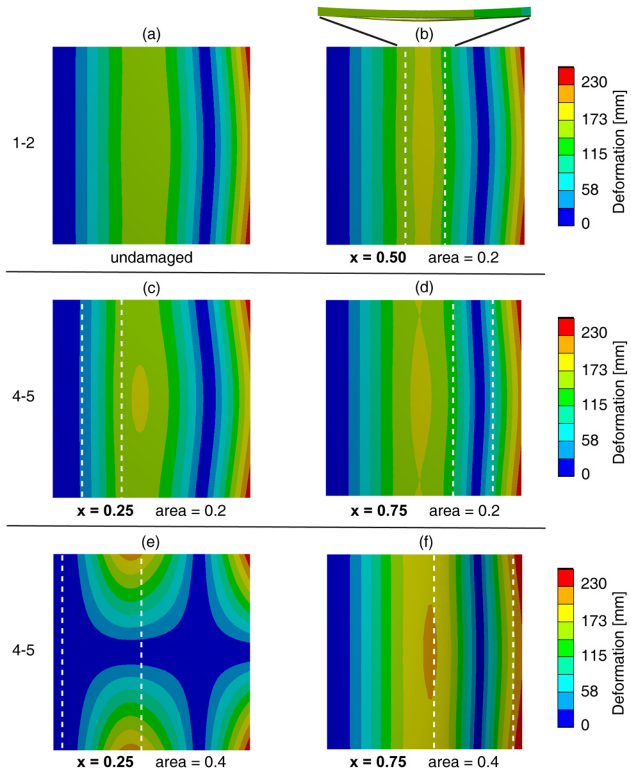

FIG. 3. Mode 4 shape for (a) undamaged plate, (b) 1–2 delamination of length 0.2 at $x = 0.50$ (with side view shown), (c) 4–5 delamination of length 0.2 at $x = 0.25$, (d) 4–5 delamination of length 0.2 at $x = 0.75$, (e) 4–5 delamination of length 0.4 at $x = 0.25$, and (f) 4–5 delamination of length 0.4 at $x = 0.75$. The edges of the delaminated regions are shown with dashed lines.

as the plots are normalized to each other. For all simulations run, no significant visual differences in modes 1 and 2 are observed between undamaged and damaged samples regardless of the size and location of delamination. Some visual differences are observed in mode 3 for very large delaminations; however, mode 4 produces the strongest qualitative results. Figure 3 shows mode 4 for (a) an undamaged sample and (b) a 1–2 delamination of length 0.2 centered at $x = 0.50$. This is the smallest delamination size for which any qualitative differences are observed. Although no differences are observed at this size for the 4–5 ply interface, there is a visible stripe in the center of the 1–2 delamination. From the side profile view, it is apparent that this stripe is the result of delamination breathing, mentioned previously. Because the 1–2 delamination is close to the surface of the material, it is able to vibrate open and closed independent of the overall modal vibration.

While no qualitative differences in mode 4 are observed for 4–5 delaminations of normalized length 0.2 at $x = 0.50$, there are noticeable effects for comparable delaminations at $x = 0.25$ and 0.75, as shown in Figs. 3(c) and 3(d). For both of these simulations, small regions of increased displacement are visible in mode 4. Unexpectedly, however, these regions do not appear at the location of the delamination but are instead roughly in the center of the sample for both. An extreme case of mode behavior being decoupled from delamination location is also shown in Fig. 3. The simulations for 4–5 delaminations of normalized length 0.4 are shown (e) at $x = 0.25$ and (f) at $x = 0.75$. The $x = 0.75$ delamination mode shape looks similar to the undamaged sample but the $x = 0.25$ delamination has a completely different mode shape with no apparent connection to the location of the delamination. The reason for this shift in shape is unknown but it implies that damage in specific key locations can have a dramatic effect on the global vibrational behavior of the structure.

D. Mode curvature

For each simulation conducted, the curvature of mode 1 is calculated. Mode 1 for the plate is pseudo-1D (i.e., displacement does not significantly vary along the y-axis), so curvature is calculated at $y = 100$ mm for consistency. Curvature for 4–5 delaminations centered at $x = 0.50$ between 0.05 and 0.4 in length are shown in Figs. 4(a)–4(d). The edges of the delamination are shown with dashed lines for clarity. Two important trends are apparent. First, although no visual differences are observed in the shape of mode 1 for delaminations of any size, small deviations in curvature are visible for delaminations as small as 0.05 in length. At a length of 0.2, these deviations become significant with negative curvature observed at some points, which cannot occur on an undamaged sample. Second, the curvature deviations are far larger for 4–5 delaminations than for 1–2 delaminations. The reason for this is unknown but may be related to differences in the cross-sectional area ratio in the delaminated region (1/1 vs 1/7). However, both 4–5 and 1–2 delaminations follow the same overall pattern with curvature peaks roughly lining up with the edges of the delaminated region.

Curvature for 4–5 delaminations of varying lengths centered at $x = 0.25$, 0.50, and 0.75 is shown in Figs. 4(e) and 4(f). The off-center delaminations follow the same curvature pattern described previously. The location of peaks in curvature corresponds to the edges of the delaminations, and the magnitude of the peaks increases with the severity of the delamination. Even the delamination of length 0.4 at $x = 0.25$, which has a dramatically different mode shape [see Fig. 3(e)], follows the expected curvature pattern. Thus, while mode shapes may be unpredictable and difficult to interpret, their underlying curvature reveals the size and location of delaminations with surprising consistency.

E. Localizing delaminations with machine learning and natural frequency

The random forest model is able to accurately predict the scale of delamination, i.e., the area and distance from the boundary condition. Figures 5(a) and 5(b) show the predicted-actual scatterplots for testing data. We plot the first three natural frequencies against area and the x-offset in Figs. 5(c) and 5(d), respectively, to demonstrate how difficult it is for a human to visually interpret this characterization method. The model performance metrics are provided in Table III, as well as benchmark results with a simple linear regression model with values normalized relative to the dimensions of the composite plate.

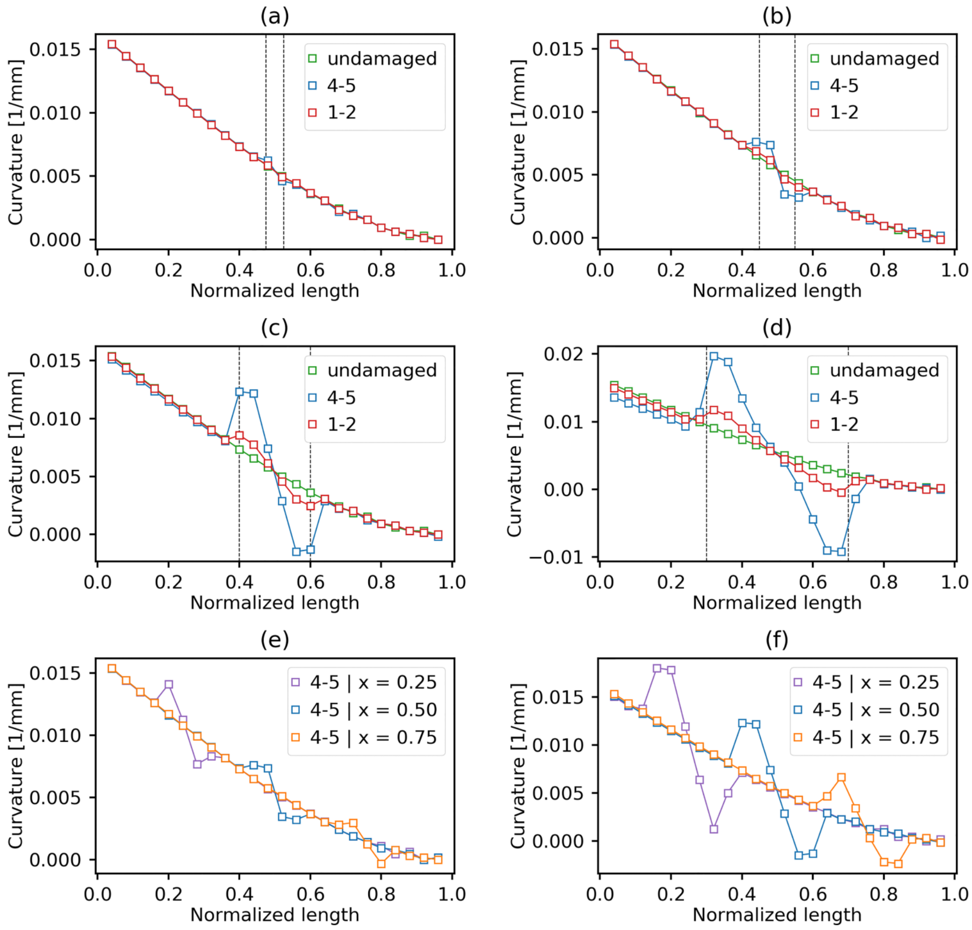

FIG. 4. (a)–(d) Mode 1 curvature for 4–5 and 1–2 delaminations of lengths 0.05, 0.1, 0.2, and 0.4, respectively, at $x = 0.50$. The edges of the delaminated region are shown with dashed lines. (e) and (f) Mode 1 curvature for 4–5 delaminations of lengths 0.1 and 0.2, respectively, centered at $x = 0.25$, 0.50, and 0.75.

IV. DISCUSSION

A. Natural frequency

The natural frequency test is the simplest vibrational test, using only a small set of natural frequency values to describe the behavior of the entire structure. A sufficient drop in natural frequency is a reliable indicator of damage;[14] however, the size of the delamination must be large in order to meet the threshold for detection. Therefore, this test is better suited to testing for significant damage already present than preemptively identifying small regions of damage before they develop. A large number of factors affect the natural frequencies of a structure, which makes it difficult to localize damage or quantify its severity, making this test level 1 without the use of machine learning.

The main advantages of the natural frequency test are its speed and simplicity—the natural frequencies of a structure can be determined with only a single force transducer and accelerometer.[38] These advantages lend themselves to two major categories of application. (1) High throughput testing on a large number of parts, for example, as a quality control measure in a factory producing composite parts and (2) large and complex systems tested *in situ* where mode shape analysis is impractical, for example, networks of composite pipes or infrastructure such as buildings and bridges.

B. Mode shape

The mode shape test is a qualitative comparison, which presents challenges to identification. The damage threshold for mode shape changes to be readily apparent to the human eye is typically high. Furthermore, damage is only observed in mode 4, which is more difficult to extract than the lower modes.[38] Higher modes typically show local behavior allowing for level 2 identification; however, our results show the difficulty of using mode shapes to reliably localize delaminations.

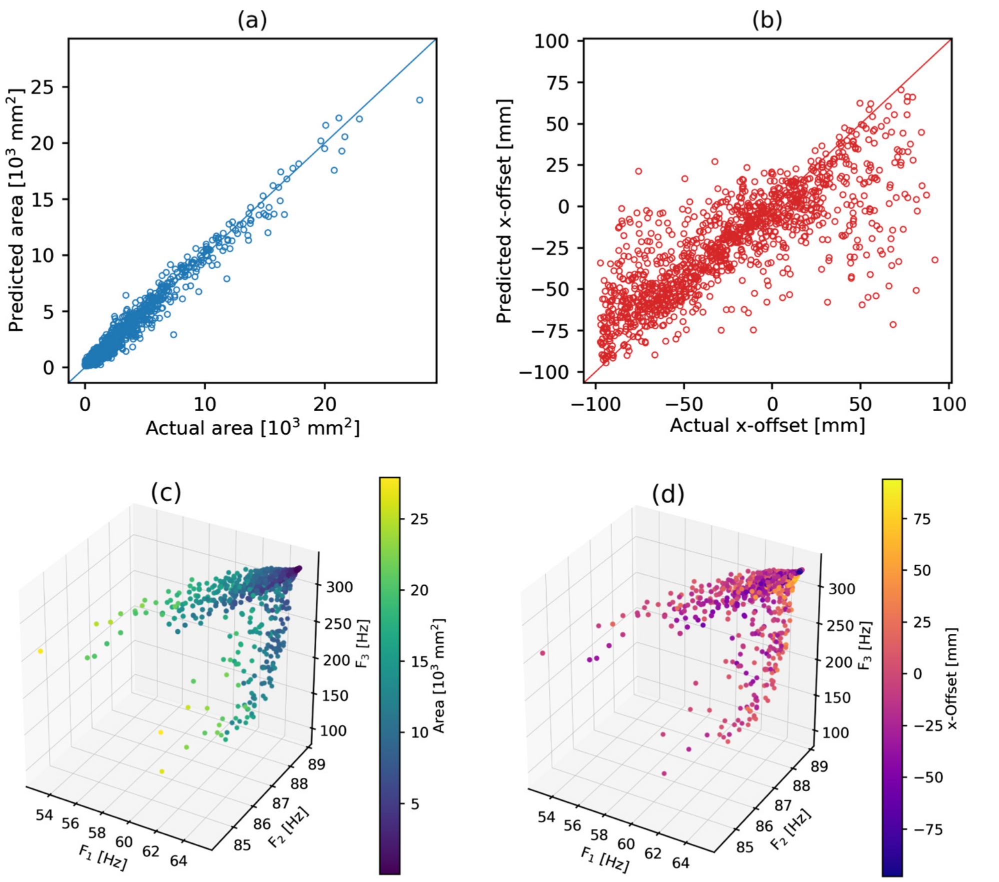

FIG. 5. The actual value vs the predicted value by the random forest model for (a) the area of the delamination and (b) the *x*-offset of the delamination, which is the distance from the center of the plate ($x = 100$ mm). The first three frequencies are plotted for (c) the area and (d) the *x*-offset of the delamination to demonstrate the difficulty of inferring the delamination properties from natural frequency through human analysis. F_x is defined as the frequency of mode *x*.

The mode shape test requires many accelerometers in order to accurately characterize the behavior of the structure; the resolution of the test is only as good as the spacing between sensors allows. Given that the complexity of setup for the mode shape test is similar to that of the mode curvature test, there is typically little incentive to use the former. The main application where mode shape seems superior is situations where damage is likely to occur just below the surface of a laminate, for example, as the result of a low velocity impact. Our results show that 1–2 delaminations are not as readily identified with mode curvature as 4–5 delaminations and instead may be easier to detect qualitatively through observation of delamination breathing. However, it is important to note that modal analysis assumes a linear structural response, and delamination breathing is an inherently nonlinear phenomenon.[9] Therefore, more experimental data are needed to verify the validity of this test.

TABLE III. Machine learning model performance for linear regression and random forest.

	Area			*x*-offset		
	MAE	MSE	R^2	MAE	MSE	R^2
Linear regression	0.027 90	0.001 430	0.828	0.1820	0.0483	0.0357
Random forest	0.009 96	0.000 227	0.974	0.0902	0.0177	0.6470

C. Mode curvature

As mentioned previously, the mode curvature test uses a similar setup to the mode shape test but requires additional data processing to reveal behavior not seen by the human eye. Our results prove the feasibility of curvature to not only detect small delaminations (1/3 the size detectable with natural frequency) but also to accurately localize and predict their severity, meaning mode curvature may allow level 3 identification. However, in practice, there are difficulties to using this test. First, mode curvature requires a large number of sensors to achieve good resolution. Replicating the results of this study experimentally would require a minimum of 26 accelerometers. Second, sensor noise is amplified in the process of numerical differentiation, which can lead to a large amount of error in curvature plots.[18] Researchers have alleviated this issue by smoothing data with spline fitting or measuring curvature directly with strain gauges.[9,18] Given the advantages and limitations of mode curvature, it is best suited to applications where identifying small delaminations is critical enough to warrant resource-intensive testing. Such applications

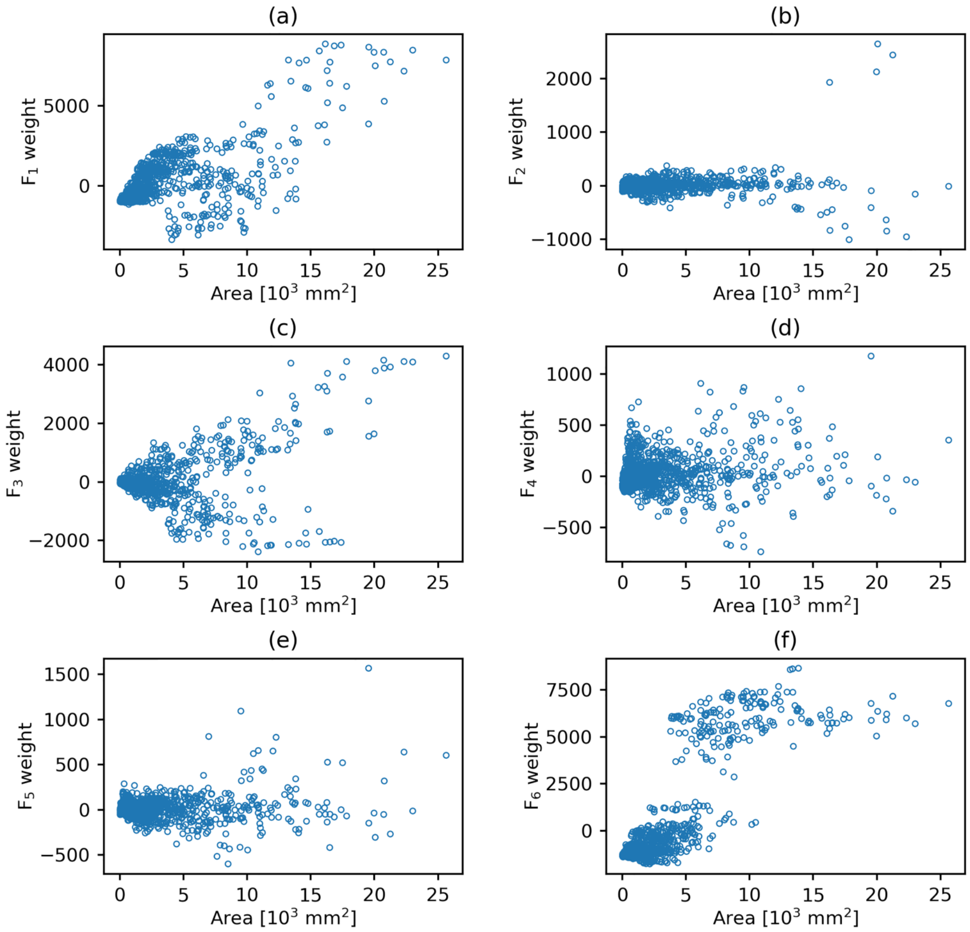

FIG. 6. Plots of the linear weights for each frequency against the area for (a) mode 1, (b) mode 2, (c) mode 3, (d) mode 4, (e) mode 5, and (f) mode 6. The data shown are from the test set to prevent overfitting. F_x is defined as the frequency of mode *x*.

may include identifying damage in aircraft bodies or ship hulls as part of routine maintenance.

D. Using and interpreting random forests

Natural frequency testing is one of the simplest non-destructive methods for detecting delamination in composites. Such non-destructive methods are particularly useful for testing novel designs of composites when evaluating their efficacy at surviving harsh conditions. We have demonstrated that a random forest model is able to accurately predict delamination. The ply interface of a delamination is also of interest for composites. However, it is found to be difficult to train a model that is able to predict the layer of the delamination with a high degree of accuracy. This suggests that the layer interface information is not adequately contained or revealed in the natural frequencies. We plan to follow up and further explore possible methods for predicting the delamination layer location in future work.

Physical insight and interpretability are also important considerations, especially as they might provide insight into the relationship between natural frequencies and delamination. Using the tree-interpreter package,[33] we are able to translate random forest predictions into a linear weighted combination of the features, i.e., the natural frequencies. In Fig. 6, the coefficients associated with each prediction are plotted against the area of the delamination. A weak positive correlation with the first natural frequency is observed, agreeing with theoretical predictions. Specifically, as delaminations increase in size, they have a greater effect on the global stiffness of the plate, which is reflected in the simple bending shape of mode 1. Mode 6 seems to have a threshold area, above which it suddenly increases in importance. To explore this observation, we examine the mode shape for a centered delamination with different area sizes. Results show that the sudden change in model weight for mode 6 is mirrored by significant changes in mode 6 shape, as shown in Fig. 7(a). At a delamination area of around 5000 mm^2, mode 6 shifts from flexion spanning the entire plate to highly localized delamination breathing. To confirm that this phenomenon is specifically predicted by the model and rule out confounding factors, a similar experiment for mode 2 is performed. As shown in Fig. 7(b), the model weight

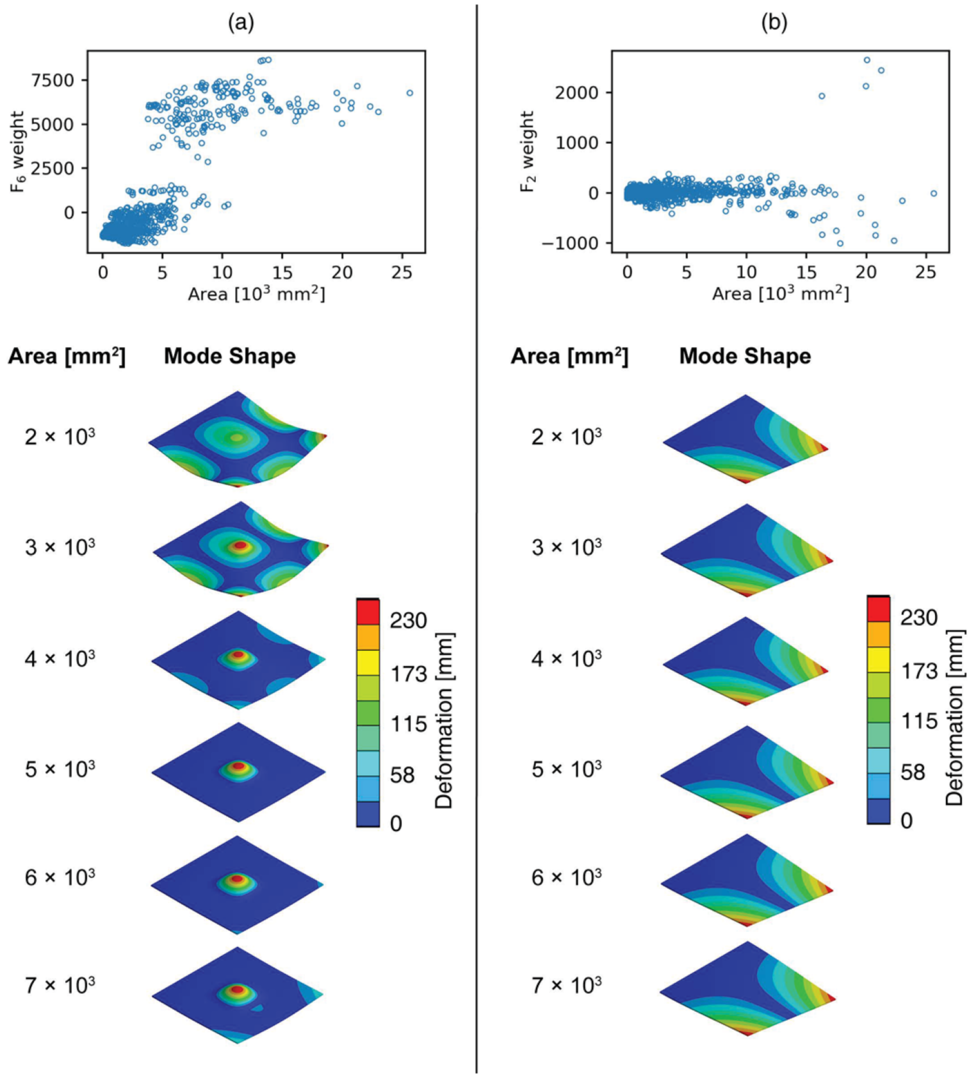

FIG. 7. (a) Mode 6 shape of centered 1–2 delamination and (b) mode 2 shape of centered 1–2 delamination showing how a change in linear weight corresponds to a transition from global to local modal behavior. F_x is defined as the frequency of mode *x*.

remains low for all delamination areas and as a result, the mode shape does not significantly change as area increases.

An additional exploration is done to examine how well the model can generalize to delamination shapes other than a rectangle. Results show that our model is able to generalize by applying our methodology to circular delaminations. Specifically, we are able to train a RF model to localize and predict the area of 400 random circular delaminations with similar accuracy as for rectangular delaminations. In addition, a similar phase transition in the model weight is observed for mode 1, and as predicted, the mode 1 shape shifts from global to localized behavior at this point.

Using machine learning for non-destructive characterization and design of composites is a largely unexplored space. In particular, our use of interpretable random forests may lend itself to many different applications. For future work, we plan to explore different delamination types, more complex composite designs, and generalization capabilities to arbitrarily shaped delaminations. We also wish to incorporate higher-order frequencies and use the interpretable machine learning methods from this paper to derive more physical insight between delamination area and natural frequencies.

V. CONCLUSIONS

Although still relatively uncommon compared to other conventional test methods, vibrational testing of composites shows promise in a variety of applications. Our work provides a more thorough picture of the range of delamination sizes and locations detectable by different test types than was previously available. Additionally, we present a machine learning method to enhance the capabilities of the natural frequency test to measure delamination damage beyond what is possible with conventional analysis. Using interpretation tools, we elucidate novel relationships between natural frequencies and mode shapes. These test methods provide a convenient way to evaluate existing composite structures as well as rapidly iterate over new materials for the design of novel high-performance composites.

ACKNOWLEDGMENTS

The authors acknowledge support from the Extreme Science and Engineering Discovery Environment (XSEDE) at the Pittsburgh Supercomputing Center (PSC) by National Science Foundation (NSF) Grant No. ACI-1548562. Additionally, the authors acknowledge support from an NVIDIA GPU Seed Grant.

DATA AVAILABILITY

The data that support the findings of this study are available from the corresponding author upon reasonable request.

REFERENCES

[1] J. Bauer, S. Hengsbach, I. Tesari, R. Schwaiger, and O. Kraft, Proc. Natl. Acad. Sci. U.S.A. **111**, 2453 (2014).
[2] C.-T. Chen, F. J. Martin-Martinez, S. Ling, Z. Qin, and M. J. Buehler, Nano Futures **1**, 011003 (2017).
[3] G. X. Gu, M. Takaffoli, and M. J. Buehler, Adv. Mater. **29**, 1700060 (2017).
[4] J. Wang, Q. Cheng, and Z. Tang, Chem. Soc. Rev. **41**, 1111 (2012).
[5] G. X. Gu, F. Libonati, S. D. Wettermark, and M. J. Buehler, J. Mech. Behav. Biomed. Mater. **76**, 135 (2017).
[6] C. N. Della and D. Shu, Appl. Mech. Rev. **60**, 1 (2007).
[7] P. H. Geubelle and J. S. Baylor, Composites Part B Eng. **29**, 589 (1998).
[8] K.-F. Nilsson, L. E. Asp, J. E. Alpman, and L. Nystedt, Int. J. Solids Struct. **38**, 3039 (2001).
[9] S. W. Doebling, C. R. Farrar, and M. B. Prime, Shock. Vib. **30**, 91 (1998).
[10] Z. Zhang, K. Shankar, E. V. Morozov, and M. Tahtali, J. Vib. Control **22**, 496 (2016).
[11] A. Rytter, Ph.D. thesis, Aalborg University, 1993.
[12] C. R. Farrar, W. E. Baker, T. M. Bell, K. M. Cone, T. W. Darling, T. A. Duffey, A. Eklund, and A. Migliori, *Dynamic Characterization and Damage Detection in the I-40 Bridge Over the Rio Grande* (Los Alamos National Laboratory, 1994).
[13] A. Żak, M. Krawczuk, and W. Ostachowicz, Comput. Mech. **26**, 309 (2000).
[14] O. S. Salawu, Eng. Struct. **19**, 718 (1997).
[15] J. Ko, C. Wong, and H. Lam, in *Proceedings of the 12th International Modal Analysis Conference* (Society for Experimental Mechanics, 1994), p. 280.
[16] J.-H. Kim, H.-S. Jeon, and C.-W. Lee, in *Proceedings of the 10th International Modal Analysis Conference* (Society for Experimental Mechanics, 1992), p. 536.
[17] A. K. Pandey, M. Biswas, and M. M. Samman, J. Sound Vib. **145**, 321 (1991).
[18] C. P. Ratcliffe and W. J. Bagaria, AIAA J. **36**, 1074 (1998).
[19] C.-T. Chen and G. X. Gu, MRS Commun. **9**, 556 (2019).
[20] A. Paul, P. Acar, W.-K. Liao, A. Choudhary, V. Sundararaghavan, and A. Agrawal, Comput. Mater. Sci. **160**, 334 (2019).
[21] C. T. Chen and G. X. Gu, Adv. Sci. **7**, 1902607 (2020).
[22] G. Pilania, C. Wang, X. Jiang, S. Rajasekaran, and R. Ramprasad, Sci. Rep. **3**, 2810 (2013).
[23] C. Yang, Y. Kim, S. Ryu, and G. X. Gu, MRS Commun. **9**, 609 (2019).
[24] Y. Rivenson, Y. Zhang, H. Günaydın, D. Teng, and A. Ozcan, Light Sci. Appl. **7**, 17141 (2018).
[25] C. Yang, Y. Kim, S. Ryu, and G. X. Gu, Mater. Des. **189**, 108509 (2020).
[26] C. T. Chen and G. X. Gu, Adv. Theory Simul. **2**, 1900056 (2019).
[27] S. Ye, B. Li, Q. Li, H.-P. Zhao, and X.-Q. Feng, Appl. Phys. Lett. **115**, 161901 (2019).
[28] L. Lu, M. Dao, P. Kumar, U. Ramamurty, G. E. Karniadakis, and S. Suresh, Proc. Natl. Acad. Sci. U.S.A. **117**, 7052 (2020).
[29] L. Bornn, C. R. Farrar, G. Park, and K. Farinholt, J. Vib. Acoust. **131**, 021004 (2009).
[30] A. Bernieri, L. Ferrigno, M. Laracca, and M. Molinara, IEEE Trans. Instrum. Meas. **57**, 1958 (2008).
[31] A. Khan, D.-K. Ko, S. C. Lim, and H. S. Kim, Compos, Part B Eng **161**, 586 (2019).
[32] L. Breiman, Mach. Learn. **45**, 5 (2001).
[33] A. Saabas, https://github.com/andosa/treeinterpreter.
[34] M.-H. H. Shen and J. E. Grady, AIAA J. **30**, 1361 (1992).
[35] J. Gere and B. Goodno, in *Mechanics of Materials*, 7th ed. (Cengage Learning, 2008).
[36] S. C. Chapra and R. P. Canale, in *Numerical Methods for Engineers*, 7th ed. (McGraw-Hill Education, 2014).
[37] F. Pedregosa, G. Varoquaux, A. Gramfort, V. Michel, B. Thirion, O. Grisel, M. Blondel, P. Prettenhofer, R. Weiss, V. Dubourg, J. Vanderplas, A. Passos, D. Cournapeau, M. Brucher, M. Perrot, and E. Duchesnay, J. Mach. Learn. Res. **12**, 2825 (2011).
[38] Z.-F. Fu and J. He, *Modal Analysis* (Butterworth-Heinemann, 2001).